Proceedings of the
Annual Stability Conference
Structural Stability Research Council
Atlanta, Georgia, April 21-24, 2026

Experimental study on the buckling behavior of aluminum members with closed cross-sectional shapes

Hoang Duong Ngoc[1], Prachi Verma[2], Sahar Dahboul[3], Pampa Dey[4], Nicolas Boissonnade[5]

Abstract

Aluminum members offer an attractive combination of low weight, corrosion resistance, and low maintenance, yet their use as primary load-bearing elements remains limited in part because current design rules do not always predict their strength and stability with sufficient accuracy. The objective of this paper is to improve the understanding of buckling behavior in extruded aluminum members with closed cross-sectional shapes and to evaluate how well current American design provisions capture their resistance. An experimental program was carried out on extruded 6061-T6 square and rectangular hollow profiles, including standard tensile coupon tests to establish material properties and careful measurements of both local and global geometric imperfections. The test series comprised four short sections loaded in concentric compression and two long members loaded in eccentric compression to represent combined compression and bending. The experiments document the observed buckling modes and ultimate resistances for each configuration, providing a benchmark dataset for assessing design methods for tubular members. When the measured resistances are compared with predictions from the Aluminum Design Manual, the design checks are consistently conservative for the specimens studied, indicating that there is scope to improve the accuracy of stability design for aluminum tubular members. The results provide a foundation for refined stability design guidance, and future work will expand the experimental database to a wider range of member slenderness, cross-section proportions, and loading eccentricities and will propose a new design methodology.

1. Introduction

Aluminum alloys are increasingly considered for structural applications because they combine a high strength-to-weight ratio with excellent corrosion resistance, durability, low maintenance requirements and full recyclability (Beaulieu and Marsh 2006). These attributes make aluminum attractive for lightweight structural systems such as bridges, modular construction, pedestrian structures, and transportation-sensitive projects where reducing self-weight can lead to savings in foundations, fabrication, handling and erection. Nevertheless, aluminum remains less widely used

[1] PhD Student, Laval University, <ngoc-hoang.duong.1@ulaval.ca >
[2] PhD Student, Laval University, <prachi.verma.1@ulaval.ca>
[3] PhD, Structural Engineer, WSP Canada Inc., <sahar.dahboul.1@ ulaval.ca>
[4] Associate Professor, Laval University, <pampa.dey@gci.ulaval.ca>
[5] Professor, Laval University, <nicolas.boissonnade@gci.ulaval.ca>

than steel in primary load-bearing systems, largely because its Young's modulus is approximately one third of that of carbon steel. The resulting lower stiffness increases sensitivity to stability phenomena, such that local plate buckling, overall member buckling, and their interaction often govern resistance rather than material strength alone.

Stability performance can be improved by adopting cross-sections with higher stiffness and favourable stability characteristics. In this context, square and rectangular hollow sections (SHS and RHS) are particularly attractive as they provide high flexural rigidity about both principal axes and benefit from the vastly superior torsional stiffness associated with closed thin-walled geometries. At the same time, their thin plate elements can be susceptible to local buckling, while moderate-to-slender members may exhibit global flexural buckling. Interaction between these modes may significantly affect the ultimate resistance. In practical structures, axial compression is rarely perfectly concentric; fabrication tolerances, load introduction details, frame deformations, and initial crookedness commonly induce combined compression and bending. For square and rectangular hollow sections (SHS/RHS) members, this may lead to uniaxial or biaxial bending in addition to axial force, making the stability problem inherently interaction based. Reliable design therefore requires resistance models that capture the governing buckling mechanisms of SHS/RHS members under eccentric compression without becoming impractical for routine engineering use.

A substantial body of experimental work has examined aluminum sections and members under pure compression or combined compression and uniaxial bending, providing insight into strength and buckling behavior and supporting the assessment of current design approaches (Liu et al. 2015; Hu et al. 2021; Yu et al. 2022; Zhao et al. 2016; Zhao et al. 2019; Zhu and Young 2006a; Zhu and Young 2006b). In contrast, experimental evidence for members under combined compression and biaxial bending remains limited, even though biaxial bending can arise in practice due to load eccentricities, member orientation, and frame effects. Additional test data under biaxial bending is therefore needed to clarify the governing instability mechanisms and to evaluate the accuracy of current design provisions for tubular aluminum members.

A further motivation for the present work is that stability design for tubular members rely on resistance components that originate at different behavioural levels. Section tests isolate section response and local instability mechanisms, providing direct information on local buckling resistance and the influence of cross-section geometry and material behaviour. Member tests, on the other hand, activate member-level stability in the presence of combined compression and bending, where global buckling and local-global interaction may control capacity. Treating both levels within a single experimental framework, with consistent material characterization and measured initial imperfections, provides a clearer basis for interpreting the observed failure modes and for benchmarking design provisions across the full stability problem.

Accordingly, the present paper reports an experimental investigation on extruded 6061-T6 aluminum tubular members with closed cross-sectional shapes, combining both section and member tests. The program includes section (stub column) tests under concentric compression and member tests under eccentric compression representative of combined compression and bi axial bending. Complementary tensile coupon tests are conducted to establish the material stress-strain response, and detailed measurements of local and global geometric imperfections are carried out to accurately characterize the initial geometry of each specimen. The resulting ultimate resistances and observed failure modes provide a benchmark to assess the accuracy of current design predictions for aluminum tubular members. In particular, the experimental capacities are compared against resistance predictions obtained from the Aluminum Design Manual (ADM) (Aluminum

Association 2020). The findings are intended to support improved stability design guidance for extruded aluminum SHS/RHS, and they form the basis for future work aimed at expanding the experimental database and proposing a new design methodology calibrated to the observed behaviour.

2. A brief background on design predictions by the Aluminum Design Manual (ADM)

The Aluminum Design Manual (ADM 2020) treats the resistance of aluminum members in compression as governed by a combination of member-level instability, cross-section local buckling, and (in thin-walled shapes) their possible interaction. Accordingly, the available axial compressive strength P_c in the Load and Resistance Factor Design (LRFD) is taken as the smallest of the corresponding nominal strengths:

$$P_c = \phi_c \cdot \min\left(P_{n,MB}, P_{n,LB}, P_{n,INT}\right) \tag{1}$$

where $P_{n,MB}$ represents the nominal strength limited by overall member buckling, $P_{n,LB}$ represents the nominal strength limited by local buckling of the plate elements forming the tube, and $P_{n,INT}$ accounts for the interaction between member buckling and local buckling when both effects are relevant. In this study, ϕ_c (strength reduction factor) is taken as 1.0 to enable a direct, "unfactored" comparison between ADM predictions and experimental peak loads. The detailed procedures used in ADM to evaluate $P_{n,MB}$, $P_{n,LB}$, and $P_{n,INT}$ including the member-strength expressions, plate-element buckling provisions, and interaction formulation are provided in the ADM (Aluminum Association 2020) and are not repeated here for brevity. For members subjected to combined axial force and bending, ADM evaluates adequacy using a linear interaction expression of the form:

$$\frac{P_r}{P_c} + \frac{M_{rx}}{M_{cx}} + \frac{M_{ry}}{M_{cy}} \leq 1.0 \tag{2}$$

where P_r is the required axial force, M_{rx} and M_{ry} are the required bending moments about the major and minor axes, and M_{cx} and M_{cy} are the corresponding available flexural strengths determined from the ADM flexural provisions (including the relevant yielding/rupture and local-buckling checks, and, where applicable, member stability effects in bending through the moment-gradient coefficient). For section tests under concentric compression, only Eq. (1) applies, whereas for member tests under eccentric compression the ADM axial resistance reported in this paper corresponds to the axial load level that satisfies Eq. (2) for the prescribed eccentricity and bending configuration.

3. Test specimens

This study presents an experimental programme on extruded 6061-T6 aluminum specimens with square and rectangular hollow cross-sections, representative of closed thin-walled members used in structural applications. Two cross-section geometries were investigated, a rectangular hollow section with overall dimensions $b = 76.2\ mm$, $h = 152.4\ mm$ and wall thickness $t = 4.8\ mm$, and a square hollow section with $b = h = 152.4\ mm$ and $t = 12.7\ mm$ as shown in Fig. 1.

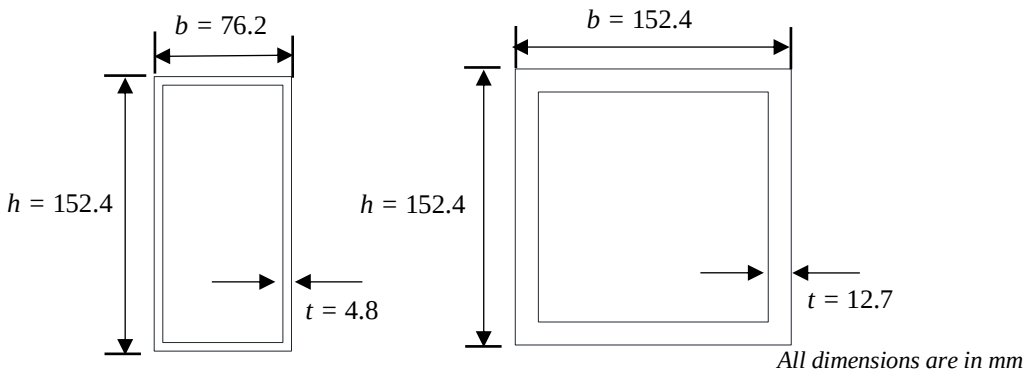

Figure 1. Section profiles investigated: RHS (left) and SHS (right).

The selection of geometries, lengths and loading conditions was designed to investigate stability behaviour at both the section and member levels. Accordingly, stub-column tests were performed under concentric compression to characterize section-dominated response and local buckling behaviour, while beam-column tests were performed under eccentric compression to represent combined compression and bending conditions typical of practical structures. The stub-column specimens had a length of 400 *mm* (approximately three times the larger cross-section dimension) to limit overall member effects, whereas the beam-column specimens were selected with moderate-to-high slenderness to activate member stability, with representative lengths of 2.7 *m* and 3.0 *m* depending on the cross-section.

For clarity and consistency throughout the paper, the specimens are designated using a concise convention that indicates both the cross-section type and the test category. The stub-column (section) tests are labelled RHS-S1 and RHS-S2 for the repeated RHS stub column tests, and SHS-S1 and SHS-S2 for the repeated SHS stub column tests. The member (beam-column) tests include one RHS member and one SHS member, labelled RHS-M and SHS-M, respectively. In the remainder of the paper, the term "sections" refers to stub-column specimens and "members" refers to beam-column specimens.

4. Preliminary measurements

Prior to structural testing, the specimens were characterized to establish their initial geometric and material properties. In particular, (i) the initial geometric imperfections were measured over the specimen surfaces through 3D scanning, and (ii) tensile coupon tests were performed to determine the actual stress-strain response and key strength parameters of the 6061-T6 alloy. These measurements provide the input data required for interpreting test behavior and, where applicable, for subsequent numerical modelling.

To characterise the material response of the tested specimens, tensile coupon tests were performed to obtain the engineering stress-strain behaviour and the key mechanical properties of the extruded 6061-T6 alloy. Coupons were prepared for both cross-section types and for both specimen categories in the test programme. In total, two coupons were taken from the RHS sections and two from the SHS sections, and similarly two coupons were taken from the RHS member specimen and two from the SHS member specimen, to verify repeatability of the measured properties within each group. The coupon geometry and preparation followed the relevant provisions of ASTM standards (ASTM, 2015) and EN ISO 377 (EN ISO 377, 1997). The coupons were extracted from representative flat plate regions of the profiles and tested on a 500 *kN* MTS hydraulic testing

machine under displacement-controlled loading. The loading protocol and rate followed recommended procedures reported in the literature (Huang and Young, 2014), and the elastic modulus was evaluated from repeated loading-unloading segments to obtain a reliable value.

The material properties reported in this paper including the Young's modulus E, the 0.2% proof stress $\sigma_{0.2}$, the 1.0% proof stress $\sigma_{1.0}$, the ultimate tensile strength σ_u and the ultimate strain ε_u are provided in Table 1 as average values for four groups: RHS-section, SHS-section, RHS-member, and SHS-member.

Table 1. Measured tensile coupon properties for the tested 6061-T6 SHS and RHS specimens.

Sections	E $[N/mm^2]$	$\sigma_{0.2}$ $[N/mm^2]$	$\sigma_{1.0}$ $[N/mm^2]$	σ_u $[N/mm^2]$	ε_u [%]
RHS-section	66 488	303.39	311.09	322.13	6.07
SHS-section	69 398	291.48	299.12	314.07	6.09
RHS-member	69363.5	290.63	304.5	326.545	6.345
SHS-member	67790.7	290.41	294.835	314.105	11.02

5. Experimental program

5.1. Load cases and specimen categories

The experimental program was designed to investigate the stability response of extruded 6061-T6 aluminum tubular profiles at both the section and member levels, using consistent material characterization and measured initial geometry. Two specimen categories were considered:

Section resistance (stub columns): stub columns were tested in concentric axial compression to emphasise section-dominated behaviour and local plate instability while suppressing global member buckling. All stub-column specimens had a length of 400 *mm*. Two repeated tests were performed for each profile and are labelled RHS-S1, RHS-S2 and SHS-S1, SHS-S2.

Member resistance (beam-columns): slender specimens were tested in eccentric compression to generate combined compression and bending representative of practical conditions. Two member tests were performed: one RHS beam-column (RHS-M) with $L = 3000$ *mm* and one SHS beam-column (SHS-M) with $L = 2700$ *mm*. For both members, the load eccentricity was $e = 65$ *mm*. Biaxial bending was introduced by rotating the specimens about their longitudinal axis, with rotation angles $\alpha = 40°$ for RHS-M and $\alpha = 45°$ for SHS-M.

5.2. Test setup and instrumentation

Stub column specimens were prepared to ensure reliable and repeatable load introduction. Specimen ends were carefully machined/ground to be flat and perpendicular to the longitudinal axis, limiting unintended bending due to end misalignment. The concentric compression tests were conducted in a high-capacity hydraulic testing frame (up to 5000 *kN*) as shown in Fig. 2. Axial shortening was measured using an LVDT mounted to record relative movement of the plates (end-shortening) during loading.

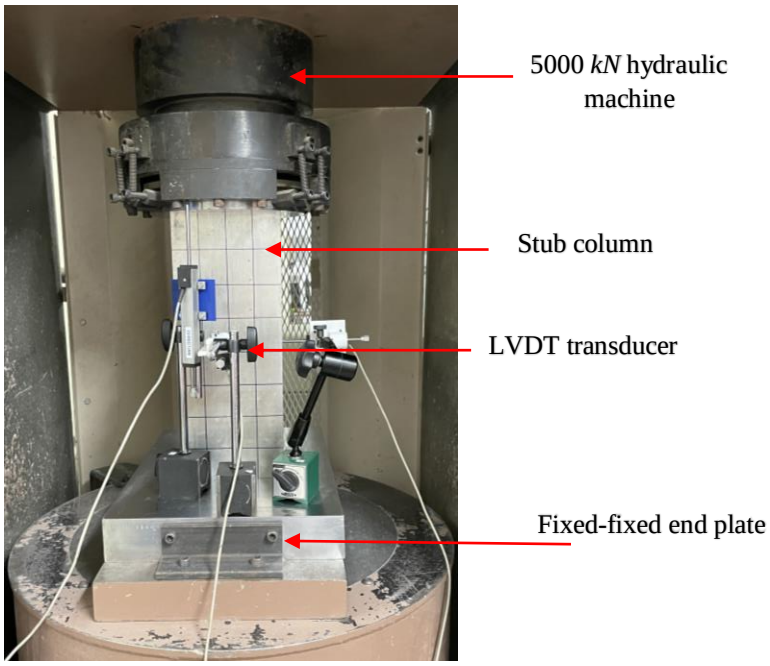

Figure 2. Test setup for section resistance test.

For member specimens, eccentric compression tests were conducted in a servo-hydraulic frame using a load cell selected according to the expected specimen resistance (2000 *kN* or 5000 *kN*) as shown in Fig. 3. The members were installed between top and bottom end plates equipped with cylindrical rollers to provide nominally pinned end conditions. Axial load transfer was achieved using a bolted clamping arrangement to avoid welding-related heat effects and to promote consistent force introduction. Steel packers were placed locally at the tube ends to reduce the risk of local crushing and to improve load transfer uniformity.

Instrumentation was selected to capture both global response and indicators of local-global interaction. End shortening was measured using LVDTs spanning between the end plates. Lateral displacement and torsional twist at mid-height were recorded using string-type displacement transducers installed on two adjacent faces. Longitudinal strain gauges at mid-height were also used to monitor axial strain development during loading.

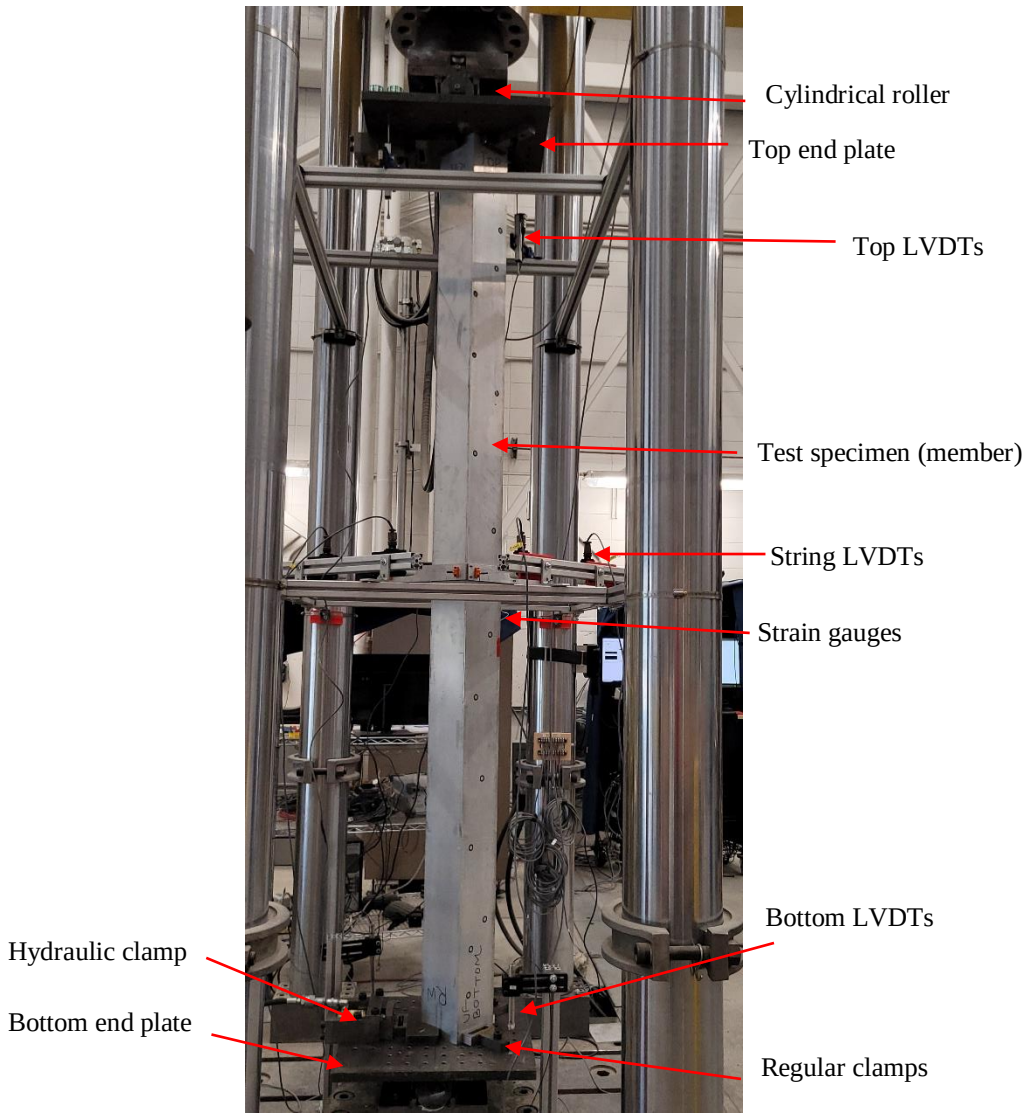

Figure 3. Test setup for member resistance test.

5.3. Loading protocol

All tests were performed under displacement control to ensure stable progression through peak resistance. For stub columns, monotonic compression was applied at a constant rate chosen to provide smooth acquisition of the local buckling response. For members, displacement-controlled loading was applied at approximately 0.3-0.4 *mm*/*min* and continued sufficiently beyond peak to clearly identify the ultimate resistance and associated instability response. For each specimen, the primary reported quantities include the peak axial load N_{exp} and the corresponding displacement measure δ_{exp} at peak. In addition, the member tests are described by the prescribed eccentricity (e) and rotation angle (α), which define the resulting combined compression and bending state used later for design comparisons.

6. Observed behavior

This section summarizes the key experimental observations from both the stub-column and beam-column tests. The focus is on identifying the governing instability mechanisms and linking them to the measured peak resistances. The results are first discussed in terms of the observed failure modes, then the ultimate resistances are presented to highlight repeatability and overall trends that support the subsequent design evaluation.

6.1. Failure mode classification

The observed responses are interpreted by distinguishing between section-dominated and member-dominated instability mechanisms. The stub-column specimens (RHS-S1/S2 and SHS-S1/S2), owing to their short length (400 *mm*) and concentric loading ($e = 0$, $\alpha = 0°$), are used to identify characteristic local plate buckling patterns in SHS/RHS profiles and to assess repeatability between the paired tests for each geometry. In contrast, the member specimens (RHS-M with $L = 3000\,mm$ and SHS-M with $L = 2700\,mm$) were tested under eccentric compression ($e = 65\,mm$) to activate member-level stability behavior under combined compression and bending. The applied rotations ($\alpha = 40°$ for RHS-M and $\alpha = 45°$ for SHS-M) introduce biaxial bending, enabling observation of global flexural buckling and the possible emergence of local plate instability in interaction with member deformations. The failure modes are classified accordingly in this section based on the dominant observed mechanism (local buckling, global buckling, or interaction), as illustrated in Fig. 4 for section specimens and Fig. 5 for member specimens.

Figure 4. Stub columns deformed shapes: RHS (left) and SHS (right).

6.2. Ultimate resistance and key trends

Ultimate resistances are summarized in terms of N_{exp} for each specimen as shown in Table 2. For the stub-column tests, repeatability is assessed by comparing the two repeated results for each profile (RHS-S1 vs RHS-S2; SHS-S1 vs SHS-S2). For the member tests, the peak resistances of RHS-M and SHS-M are reported alongside their loading descriptors (L, e, and α) to support interpretation of the governing behaviour under eccentric compression with biaxial bending. These experimental resistances and mode classifications form the basis for the subsequent evaluation of ADM design predictions.

Figure 5. Members deformed shapes: RHS (left) and SHS (right).

7. Comparison with design resistances predicted by the ADM

Table 2 compares the experimental peak loads N_{exp} with the corresponding predictions N_{ADM} obtained from the Aluminum Design Manual (ADM, 2020). The ADM values were calculated using the LRFD equations with the measured material properties from coupon tests and the measured geometric properties of the specimens. To enable a direct, model-to-test comparison, the safety factor was taken as $\phi = 1.0$ (i.e., no strength reduction was applied), so that differences primarily reflect prediction accuracy rather than design conservatism. The comparison is expressed through the ratio N_{exp}/N_{ADM}, together with the observed governing failure mode (L = local buckling; G = global buckling; L+G = interaction).

Across all six tests, the ratios N_{exp}/N_{ADM} range from 1.04 to 1.19, indicating that the ADM predictions are conservative for every specimen in this programme. The mean ratio over the full dataset is 1.10, corresponding to an average under-prediction of approximately 10% relative to the measured peak loads. Coefficients of variation are reported close to 5%.

For the stub-column (section) tests, all specimens were governed by local buckling (L). The ratios fall between 1.04 and 1.13, with a mean value of 1.07 (C.o.V. ≈ 4%). The repeated RHS stub tests yield very similar resistances and ratios, while the SHS repeats exhibit a larger difference, which is consistent with the sensitivity of local plate buckling to minor variations in initial geometry and test conditions.

For the member tests, the ratios are 1.19 for RHS-M and 1.12 for SHS-M (mean 1.16, C.o.V. ≈ 4%), suggesting a higher level of conservatism for the member-level stability cases in this limited dataset. Both member tests were conducted under eccentric compression with biaxial bending (defined by $e = 65\ mm$ and specimen rotations $\alpha = 40°$ for RHS-M and $\alpha = 45°$ for

SHS-M). The RHS-M test developed local-global interaction (*L+G*) and was carried out with a triangular bending moment distribution, whereas the SHS-M response was governed primarily by global buckling (*G*) and was conducted under a constant bending moment distribution. While the present member dataset is limited, the results indicate that interaction effects and moment distribution may influence the level of conservatism observed in the ADM checks. However, these effects are coupled with differences in cross-section geometry and rotation angle and should therefore be examined further.

Overall, the comparisons show that, when evaluated using measured properties and $\phi = 1.0$, the ADM provides safe resistance predictions for the tested extruded SHS/RHS sections and members, with a consistent tendency toward conservatism particularly for the member specimen cases under combined compression and biaxial bending.

Table 2. Experimental results and ADM predictions for section and member specimens.

Specimens	Type	Loading	Failure	N_{exp}	δ_{exp}	N_{ADM}	N_{exp} / N_{ADM}
	[–]	[–]	[–]	[*kN*]	[*mm*]	[*kN*]	[–]
RHS-S1	Section	Compression	*L*	529.40	2.25	503.81	1.05
RHS-S2	Section	Compression	*L*	522.90	5.80	502.88	1.04
SHS-S1	Section	Compression	*L*	2403.05	17.80	2126.55	1.13
SHS-S2	Section	Compression	*L*	2200.80	17.30	2076.42	1.06
RHS-M	Member	Compression + biaxial bending	*L+G*	157.00	13.36	132.15	1.19
SHS-M	Member	Compression + biaxial bending	*G*	716.20	15.66	638.89	1.12

8. Conclusions and future work

This study reported experimental tests on extruded aluminum tubular specimens with square and rectangular hollow cross-sections to examine stability behaviour at both the cross-section level and the member level. Short section specimens were tested in concentric compression, and longer member specimens were tested in eccentric compression with bending.

The main conclusions are:

- The short specimens failed by local buckling. Repeat tests showed good overall consistency, with some scatter that is typical for thin-walled local buckling behaviour;
- The longer specimens failed by member instability under combined compression and bending. One test showed interaction between local buckling and overall member buckling, while the other was governed primarily by overall member buckling:
- When the design predictions were compared with the experimental peak loads using the measured material and geometric properties and without applying a resistance factor, the design method gave conservative resistance predictions for all tests.

Future work will extend the experimental database to additional cross-section sizes, wall slenderness values, member lengths, and loading conditions. The expanded database will be used to develop and calibrate a new design methodology for aluminum tubular members.

Acknowledgments

We gratefully acknowledge the financial support of the Fonds de recherche du Québec-Nature et technologies (FRQNT). We also thank our industry partner, MAADI Group Inc., for supplying the test specimens.

References

Aluminum Association. (2020). "Aluminum design manual". *Aluminum Association, Washington, D.C, USA.*

Beaulieu, D. Marsh, C. (2006). "Design of Aluminum Structures" *Presses de l'aluminium: Québec, QC, Canada*

European standard EN ISO 377. (1997). European Committee for Standardization, Central Secratariat: rue de Stassart 36, B-1050 Brussels, ICS 77.040.10; 77.140.01.

Huang, Y., Young, B. (2014). "The art of cold-formed steel and aluminium alloy coupon tests." *In Proceedings of the 7th European Conference on Steel and Composite Structures*, Naples, Italy.

Liu, M., Zhang, L., Wang, P., Chang, Y. (2015). "Experimental investigation on local buckling behaviors of stiffened closed-section thin-walled aluminum alloy columns under compression." *Thin-Walled Structures* 94, 188–198. https://doi.org/10/f7mv44

ASTM—American Society for Testing and Materials. (2015). "Standard Specification for Aluminum-Alloy Permanent Mold Castings". *ASTM International: West Conshohocken*, PA, USA ASTM B108-15.

Yu, Z., Ren, F., Ma, H., and Zhang, A. (2022). "Experimental study and numerical analysis on bearing capacity of 6082-T6 aluminum alloy columns under eccentric compression at elevated temperatures." *Structures*, 35: 1219–1231.

Zhao, Y., Zhai, X., and Sun, L. (2016). "Test and design method for the buckling behaviors of 6082-T6 aluminum alloy columns with box-type and L-type sections under eccentric compression." *Thin-Walled Structures*, 100: 62–80.

Zhao, Y., Zhai, X., and Wang, J. (2019). "Buckling behaviors and ultimate strengths of 6082-T6 aluminum alloy columns under eccentric compression – Part I: Experiments and finite element modeling." *Thin-Walled Structures*, 143: 106207.

Zhu, J.-H., and Young, B. (2006a). "Tests and design of aluminum alloy compression members." *Journal of Structural Engineering*, 132 (7): 1096–1107.

Zhu, J.-H., and Young, B. (2006b). "Experimental investigation of aluminum alloy thin-walled tubular members in combined compression and bending." *Journal of Structural Engineering*, 132 (12): 1955–1966.